Molecular Dynamics Studies of Bacteriorhodopsin's Photocycles

KLAUS SCHULTEN,* WILLIAM HUMPHREY, ILYA LOGUNOV, MORDECHAI SHEVES,† DONG XU
Beckman Institute and Departments of Physics and Biophysics, University of Illinois at Urbana-Champaign, 405 North Mathews, Urbana, Illinois 61801, USA

(Received 15 June 1995 and in revised form 25 October 1995)

Abstract. The availability of the structure of bacteriorhodopsin from electron microscopy studies has opened up the possibility of exploring the proton pump mechanism of this protein by means of molecular dynamics simulations. In this review we summarize earlier theoretical investigations of the photocycle of bacteriorhodopsin including relevant quantum chemistry studies of retinal, structure refinement, molecular dynamics simulations, and evaluation of pK_a values. We then review a series of recent modeling efforts which refined the structure of bacteriorhodopsin adding internal water, and which studied the nature of the J intermediate and the likely geometry of the K_{590} and L_{550} intermediates (strongly distorted 13-*cis*) as well as the sequence of retinal geometry and protein conformational transitions which are conventionally summarized as the M_{412} intermediate. We also review simulations of the photocycle of light-adapted bacteriorhodopsin at T=77 K and of the photocycle of dark-adapted bacteriorhodopsin, both cycles differing from the conventional photocycle through a nonfunctional (pure 13-*cis*) retinal geometry of the corresponding K_{590} and L_{550} states. The simulations demonstrate a potentially critical role of water and of minute reorientations of retinal's Schiff base nitrogen in controlling proton pumping in bR_{568}; the simulations also indicate the existence of heterogeneous photocycles. The results exemplify the important role of molecular dynamics simulations in extending investigations on bacteriorhodopsin to a level of detail which is presently beyond experimental resolution, but which needs to be known to resolve the pump mechanism of bacteriorhodopsin. Finally, we outline the major existing challenges in the field of bacteriorhodopsin modeling.

INTRODUCTION

Bacteriorhodopsin (bR) is a transmembrane protein which spans the cell membrane of *Halobacterium halobium* and functions as a light-driven proton pump. The protein contains seven α-helices which enclose the prosthetic group, the chromophore all-*trans*-retinal, bound via a protonated Schiff base linkage to Lys-216. The structure of bR is presented in Fig. 1a. Figure 1b shows the chemical structure of retinal and its conventional numbering scheme, to which we will refer in this review. Retinal absorbs light and undergoes a rapid photoisomerization process; the thermal reversal of this process is coupled to the vectorial transfer of a proton from the cytoplasmic side (top in Fig. 1a) to the extracellular side (bottom in Fig. 1a) of bR. The proton transfer serves to generate a transmembrane potential which drives the metabolism of *Halobacterium halobium*, in particular, under anaerobic conditions. Recent reviews which discuss the structure and function of bR are furnished in refs 1–7.

Even though bR is a relatively small protein, encompassing 248 amino acids, it combines for its function a multitude of properties: it is a pigment, i.e., it absorbs light and undergoes an efficient photoprocess; it pumps protons, undergoing a cyclic reaction process; the consecutive reaction steps in the proton pump cycle extend from extremely fast (500 fs for the initial photoisomerization) to slow (the complete cycle requires a few milliseconds). Bacteriorhodopsin's most intrigu-

*Author to whom correspondence should be addressed.
†Permanent address: Department of Organic Chemistry, The Weizmann Institute of Science, Rehovot 76100, Israel.

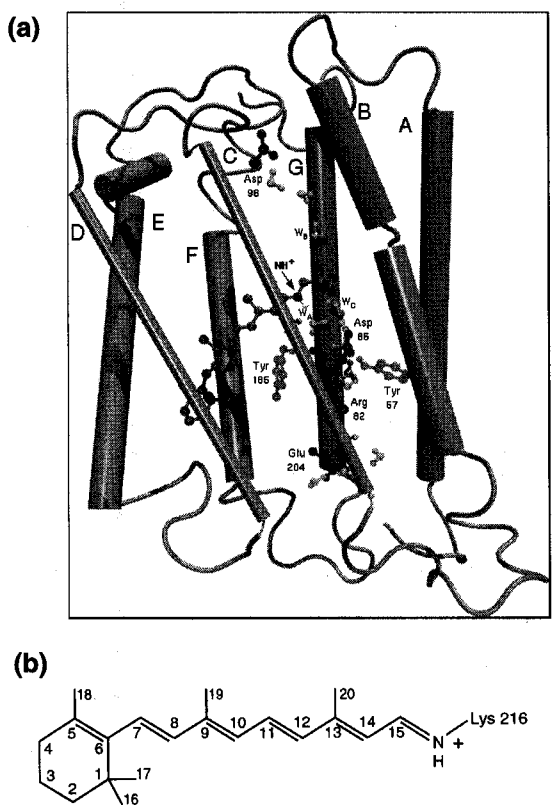

Fig. 1. (a) Ribbon diagram of bacteriorhodopsin, showing residues which are implicated in the proton pump mechanism. Water molecules placed within the protein interior are represented as solid spheres. Helices C and D are shown as thin ribbons to reveal the retinal binding site. (b) Numbering scheme of the retinal chromophore bound via a protonated Schiff base linkage to a lysine side chain.

ing attribute might be that it has resisted a two-decade-long intense research effort and not revealed the riddle of its pump mechanism.

The extracellular and cytoplasmic channels which are apparent in the structure of bR[8,9] conduct protons and form inlets and outlets for the protons pumped by bR. Even though conduction in these channels is interesting in its own right, it is passive and does not require light energy; the two channels of bR constitute solely the necessary "plumbing" of the pump, but do not explain the mechanism of the proton pump in bR, contrary to the claim in ref 10. In the present review we focus on the issue of how, through the action of light, protons are transferred irreversibly between the cytoplasmic and the extracellular channels. We will argue that the irreversible transfer of protons involves a highly specific stereochemical reaction of the Schiff base of retinal, for which motions on an Å scale and reorientations on a scale of ten degrees are crucial. Such detailed motions, the exact nature of which presently defies experimental observation, can be investigated by means of molecular dynamics (MD) studies; we will report here the considerable progress achieved.

Bacteriorhodopsin accomplishes its function through a cyclic process initiated by absorption of a photon and involving several intermediate states, labeled by letters J, K, etc. and identified by the maxima of the respective absorption spectra, e.g., 568 nm. An accepted kinetic scheme for this cycle is an unbranched series of intermediates shown in Fig. 2a. Photoisomerization occurs in the $bR_{568} \rightarrow J_{625}$ transition. During the $L_{550} \rightarrow M_{412}$ transition a proton is transferred from the Schiff base linkage of retinal to the side group Asp-85 and, subsequently, to the outside of the cell.[11-16] During the $M_{412} \rightarrow N_{520}$ transition, retinal's Schiff base again receives a proton, however from the side group Asp-96, which in turn takes up a proton from the cytoplasmic environment.[16] The reaction cycle is completed as the protein returns to bR_{568} via the O_{640} intermediate having achieved, thus, the transmembrane proton transfer.

When bR remains in the dark, it converts within an hour to a 2:1 mixture containing 13-*cis*-retinal and all-*trans*-retinal.[17] The protein containing the 13-*cis*-retinal isomer of bR absorbs at 548 nm, and is referred to as the dark-adapted (DA) pigment of bR (bR_{548}). bR_{548} contains, actually, retinal in a 13-*cis*, 15-*syn* geometry, as suggested first in ref 18 and observed in refs 19–21. bR_{548} undergoes also a reaction cycle initiated by absorption of a photon which, however, does not result in vectorial proton translocation. For recent reviews, see refs 1,2,4–6.

Numerous spectroscopic methods (absorption, fluorescence, FTIR, resonance Raman, NMR, circular, and

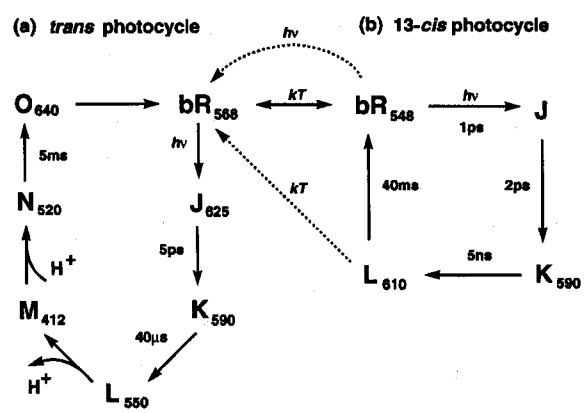

Fig. 2. Photocycles of bacteriorhodopsin. Shown are the bR_{568} (*trans*) and bR_{548} (13-*cis*) photocycles, as well as a possible connection between the two photocycles.

linear dichroism) have been employed to determine the protonation states of bR's amino acid side group involved in the proton translocation, e.g., of Asp-85 and Asp-96, as well as to identify the geometry of retinal during the photocycle.[22–28] Measurements of charge shifts have determined the kinetics of the proton transfer reactions as well as dielectric relaxation times during the photocycle.[7,29] Mutagenesis studies have played a major role in the study of bR and have allowed researchers to pinpoint the side groups participating in the various stages of the bR photocycles (see, e.g., refs 1, 30, 31).

A widely accepted model for the three-dimensional structure of bR_{568} has been provided by Henderson and coworkers on the basis of low-temperature electron-microscopy[8,9]and bR's amino acid sequence.[32,33] The observations resulted in a structure for the membrane-spanning helical portion of bR_{568} at a resolution of 3 Å in a direction parallel to the membrane and at a resolution of 10 Å perpendicular to the membrane. This structure has provided an opportunity to explore at the atomic level, by means of MD simulations, the mechanism of bR's light-driven proton pump. Such simulations can serve to refine protein structures, sample conformational states, and simulate picosecond-to-nanosecond reaction processes.[34–38] Related electrostatic calculations allow one to study solvation effects as well as to calculate pK_a values of titratable groups.[39–42]

One can formulate four principal goals for MD simulations of bR. First, atomic structures of the existing models of bR_{568} and its photointermediates need to be refined to an extent which will allow quantitative prediction of the experimentally observed spectral and kinetic characteristics of bR_{568}; this goal involves in particular the placement of waters inside bR_{568}. A second goal is the quantum chemical calculation of the excited-state potential surfaces and the simulation of bR_{568}'s photodynamics on the resulting surfaces. A third goal is the identification of the exact conformation of retinal, of internal waters, and of the protein matrix in the K_{590} intermediate which initiates the proton pump cycle. A fourth, overall goal is the elucidation of the coupling of the thermal back-reaction $K_{590} \rightarrow bR_{568}$ to vectorial proton transfer. Naturally, one hopes that the structural and functional concepts learned in achieving the stated goals can be applied towards the understanding of halorhodopsin (hR), sensory rhodopsin (sR), the visual pigments, and other bioenergetic proteins, e.g., towards the elucidation of the proton pumping mechanism in cytochrome *c* oxidase.[43]

In this review we present recent investigations of the structure and the photocycles of bR_{568} and bR_{548} which rely mainly on MD simulations. We review the state of the art of such calculations as well as illustrate the important role of the theoretical investigations. Most importantly, we wish to show that atomic level descriptions of bR's function raise new and interesting intellectual topics. We hope that these worthy issues will convince other theoretical researchers that retinal proteins pose important, challenging, and exciting problems.

EARLY THEORETICAL STUDIES OF BACTERIORHODOPSIN

Before the establishment of the structure of bR,[9] the two most important discoveries concerning bR identified retinal as the chromophore in this protein[44] and light-driven proton pumping as its function.[45] At the time of these discoveries retinal had already attracted the attention of theoretical investigators due to its essential role as the chromophore in the visual pigments (see, for example, refs 46,47).

Electronic Structure of Retinal

The theoretical studies of retinal's electronic properties and potential surfaces for nuclear motion were pioneered in the studies of Warshel and Karplus.[46,48,49] In ref 46, Warshel and Karplus explained successfully the broadness of retinal's absorption spectrum as well as its underlying vibrational structure. In ref 48, the possible role of the protein charge environment in controlling the isomerization process of in situ retinal was examined; furthermore, the bicycle-pedal model, involving simultaneous isomerization around two neighboring double bonds, was suggested as a first step in the series of the photoinduced transformations of retinal. Although possible in principle, photoinduced isomerizations around two double bonds are a rather rare event from today's perspective.[50–54] However, the bicycle-pedal motion is now an accepted mechanism for the thermally-activated dark-adaptation process in bR.[18–20,54] Following the publication of the structure of bR,[9] an attempt was made to study the dynamics of the primary photoevent in bR_{568} by treating the excited-state potential surface of in situ retinal with QCFF/PI quantum mechanical methods.[55]

Spectral Shifts and Bond Strength of Retinal

Schulten and coworkers focused their initial work also on retinal. They discovered low-lying singlet excitations in polyenes which arise due to strong electron correlation in the conjugated π-electrons.[47,56,57] The experimental and theoretical work on polyene electronic excitations is reviewed in refs 58,59. Correlation effects are governing also the strong bathochromic shifts which the spectrum of retinal experiences upon change of its environment, e.g., upon binding to bacterio-opsin, and which, hence, need to be accounted for in any descrip-

tion of the spectrum of retinal pigments and their excited-state dynamics.[60,61] Unfortunately, this requires quantum chemical calculations at a level which could not be realized for a long time for chromophores the size of retinal or its analogues. However, such calculations are becoming feasible today; a first study of this type has been completed.[62]

The extreme bathochromic shifts of retinal are accompanied by equally impressive shifts in ground-state properties. In fact, as the spectrum of retinal is red-shifted, its pattern of single and double bonds changes such that torsional barriers for double bonds decrease strongly and barriers for single bonds increase. This makes it possible for retinal to thermally isomerize around its double bonds in bR, a property which has been described.[18,63] For example, on the basis of this finding it had been suggested[18] that the dark-adaptation of bR involves isomerization around both the C_{13}–C_{14} and C_{15}–N double bonds of retinal. Most important is the realization that for the thermal back-isomerization to occur, the retinal Schiff base linkage in bR must first become protonated.[11]

The variation of the torsional barriers of retinal's single bonds through protonation and interaction with charged groups in the retinal binding site makes the single bonds, in particular the C_{14}–C_{15} bond, nontrivial participants in the geometrical transformations of retinal during bR's pump cycle. A role of single bond torsions had been originally suggested,[11,18,64] and is borne out in recent MD simulations which suggest that a pure all-*trans* → 13-*cis* photoisomerization as the initial reaction step leads actually to a nonpumping reaction cycle.[65]

Vibrational Structure of Retinal

Vibrational spectroscopy has long been held as the ideal method to identify the geometry of retinal during the photocycles of bR. Numerous investigations have successfully assigned retinal geometries to intermediates, e.g., to N_{520},[66] to O_{640},[67] and to bR_{548}.[19,68] The geometries of the M_{412} and earlier intermediates have been demonstrated to involve a 13-*cis* configuration, but assignment of further details of these geometries, in particular, the participation of single-bond torsions, has been debated.[69,70] The difficulty arises since such assignment hinges on the identification of vibrational bands and a unique relationsip between retinal's geometry and the frequency/intensity of those bands, as observed in resonance Raman and infrared spectroscopy. The strong effect of the charge environment in bR on the electronic structure and, thereby, on the vibrational modes of retinal and the geometrical flexibility of retinal in bR with numerous energetically possible geometries makes interpretations of vibrational spectra problematic. This issue has been investigated systematically,[71] with semiempirical quantum chemical methods employed to determine the vibrational frequencies of Schiff base retinal and their dependencies on the chromophore's geometry and the protein environment. The result of the investigation in ref 71 has been mainly negative in regard to the possibility of identifying torsions around retinal's C_{14}–C_{15} single bond through vibrational spectroscopy. This result lends weight to the application of MD simulations of bR's photocycle for an identification of retinal's geometries.

First Refinement of bR_{568}

The structure of bR in ref 9 resolved the key amino acid side groups involved in the proton conduction pathway, but had shortcomings which precluded a straightforward use in atomic level modeling of the proton pump mechanism. For example, the structure in ref 9 did not include the interhelical loops which extend outside the bacterial membrane. More importantly, the study in ref 9 did not resolve internal water molecules, which are essential for the conduction of protons in bR.

Internal water molecules and the retinal chromophore in bR were probed in other experiments, such as neutron diffraction, X-ray crystallography, and solid-state ^2H NMR studies. Neutron diffraction studies of deuterated bR_{568} agree with the structure reported in ref 9 in terms of the positions of many of the helical components of bR.[72–74] Neutron diffraction also verified the presence of water in the protein interior.[75] Retinal, which forms a Schiff base linkage with Lys-216, appears in the structure in ref 9 roughly at the midpoint of the proton transfer channel. Neutron diffraction revealed an orientation of retinal at a 20° angle with respect to the plane of the membrane.[76] X-ray crystallography studies produced equilibrium parameters for bond, angle, and torsional motions of retinal.[77] Solid-state ^2H NMR studies demonstrated that retinal's polyene backbone is slightly curved, its methyl groups tilting away from the membrane normal.[27]

Although no single experiment provides a complete atomic-level picture of bR, enough complementary experimental data exist to allow the use of MD to refine the structure of bR. A first refinement of the structure of bR_{568} by Nonella et al.[78] was carried out soon after the publication of the structure by Henderson et al.[9] This refinement determined the experimentally unresolved helix-connecting loop segments using a constrained simulated annealing technique; the protein was heated to 2000 K and cooled to 300 K while constraining the helical portion of the structure. The CH_3 moieties were treated as single "united" atoms in order to reduce the computational complexity of the simulation, and no wa-

ter molecules were included. This atomic level model of bR also provided the opportunity to study how steric interactions between retinal and surrounding residues affected different initial photoisomerization pathways.

Modeling of the Complete Pump Cycle

A first simulation of the complete photocycle was accomplished in the study by Zhou et al.[79] departing from the united-atom model of bR_{568} in Nonella et al.[78] The study in ref 79 followed a single trajectory through the intermediate steps of the photocycle. The overall simulation lasted only 100 ps, the reaction cycle being enforced through proton transfer from the retinal Schiff base to Asp-85, replacement of this proton through transfer from Asp-96, and lowering of the isomerization barrier of retinal's C_{13}–C_{14} bond to speed up the thermal 13-*cis* → all-*trans* reisomerization of retinal. The calculations carried out proved the feasibility of MD studies of bR_{568}'s photocycle; however, the short timescale explored and the lack of an ensemble average limited the value of this study.

In lieu of an accurate excited-state potential surface, a simple model potential for the torsional angles of the C_{13}–C_{14} and C_{14}–C_{15} bonds was employed in ref 79 to induce the all-*trans* → 13-*cis* photoisomerization. For this purpose the ground-state potential E_i^{dihe} for torsion about a bond i (the dihedral angle energy) was modified and described by the expression

$$E_i^{dihe} = \frac{1}{2} k_i [1 + \cos (n_i \phi_i + \delta_i] \qquad (1)$$

Here k_i is the energy barrier for rotation, n_i is the periodicity, ϕ_i is the torsion angle, and δ_i is a phase factor. The ground-state potential (1) for the relevant degree of freedom, torsion around the the C_{13}–C_{14} bond, conventionally is chosen with minima at both the *trans* ($\phi_i = 180°$) and *cis* ($\phi_i = 0°$) positions, i.e., with $n_i = 2$ and $\delta_i = \pi$.

Photoexcitation of bR_{568} was modeled through a sudden change to a potential

$$E_{13\text{–}14}^{dihe} = \frac{1}{2} k^* [1 + \cos (\phi_i)] \qquad (2)$$

which has a single minimum at the 13-*cis* position and a maximum at the all-*trans* position; the value of k^* was chosen to place the energy maximum at a value approximately equal to the energy of a 568-nm photon. We refer to this description of the photoisomerization as the 13-*cis* model. To describe similarly a 13,14-di*cis* model, the barrier for rotation about the C_{14}–C_{15} bond was lowered in the excited state from its ground-state values of 10 kcal/mol to an excited-state value of 2 kcal/mol. The excited-state model potentials were switched on for a period of 0.5 ps, after which the ground state potentials were restored.

The simulations by Zhou et al.[79] considered both bR structures with and without water in the protein interior. The stated model potentials induced two photoreactions of retinal, an all-*trans* → 13-*cis*,14-*trans* reaction, as suggested in refs 66,80, and an all-*trans* → 13,14-di*cis* reaction, as suggested in refs 11,18,70,81,82. The simulations indicated a preference for the 13,14-di*cis* reaction in the structure of bR used, and highlighted the importance of the electrostatic interactions between the Schiff base and its counterion in steering this reaction. Simulations with water molecules suggested the possibility of water forming a chain in the cytoplasmic channel along which a proton can be transferred from Asp-96 to the retinal Schiff base.

Second Refinement of bR_{568}

Humphrey et al.[83] furnished an improved refinement of the structure of bR_{568}, which is shown in Fig. 1a. These authors adopted an all-atom representation of bR_{568} based on the results in ref 78, but with helix D shifted by 3 Å toward the cytoplasmic side of the membrane. They placed 16 water molecules into bR, adopting a placement similar to that in ref 79. A significant amount of experimental data now exists on the importance of water in stabilizing the structure of bR, and in contributing to the photocycle dynamics, which are consistent with the MD simulations. Neutron diffraction,[75] vibrational,[84,85] and ^{15}N NMR[86] data indicate the presence of bound water within the retinal binding site. The involvement of water in stabilizing the protonated Schiff base was suggested by Dupuis et al.,[87] and the possibility has been suggested that water molecules participate in proton transfer from Asp-96 to the Schiff base.[9,88] It has been suggested also that water plays an important role in maintaining the high pK_a of the Schiff base and the low pK_a of Asp-85 in the native pigment.[89,90] Fourier-transform infrared (FTIR) data demonstrated changes in the water structure during the photocycle[91] and suggested, in particular, that a weak hydrogen-bond forms between a water molecule and the Schiff base in bR_{568} and in the L_{550} intermediate, but does not arise in a D85N mutant.[92] On the basis of this information, water molecules were placed in hydrophilic regions of the bR interior which could accommodate the water, and which were proximate to functionally important residues: above the Schiff base toward the cytoplasmic side, in the Schiff base counterion region, and below the Schiff base toward the extracellular side. Sixteen water molecules, a number close to that observed experimentally (11 ± 4),[75] fit well within these regions in a stable configuration.

As shown in Fig. 3, the water molecules placed within the bR interior in ref 83 form a complex network of hydrogen bonds within the retinal binding site, interacting with the nearby hydrophilic charged and polar residues (Arg-82, Asp-85, Asp-212, Tyr-57, Tyr-185, and others) and participating in the Schiff base counterion complex. Weak electrostatic interactions between the Schiff base and its counterion contribute also to the spectral shift (so-called opsin shift) which retinal experiences upon binding to bacterio-opsin. Water molecules within the binding site bridge the Schiff base linkage and its negatively charged carboxylate neighbors and, according to the simulations in ref 83, maintain a relatively large distance between the Schiff base and residues Asp-85 and Asp-212 of 6.0 Å and 4.6 Å, respectively. The distances are considerably larger than the respective distances of 4.1 Å and 3.7 Å in the structure of bR,[9] and are in keeping with a weak electrostatic interaction reflected in the relatively small opsin shift of bR_{568}.[61]

Experiments by Ottolenghi and Sheves[93] have measured the shift in the bR absorption maximum upon replacement of retinal by modified chromophores. The structure in ref 83 was modified accordingly, and the resulting bR structures correlated satisfactorily with the observed spectroscopic shifts between wild-type bR and bR containing the retinal analogues. This result suggests that the refined structure in ref 83 exhibits satisfactory retinal-protein sterical and electrostatic interactions.

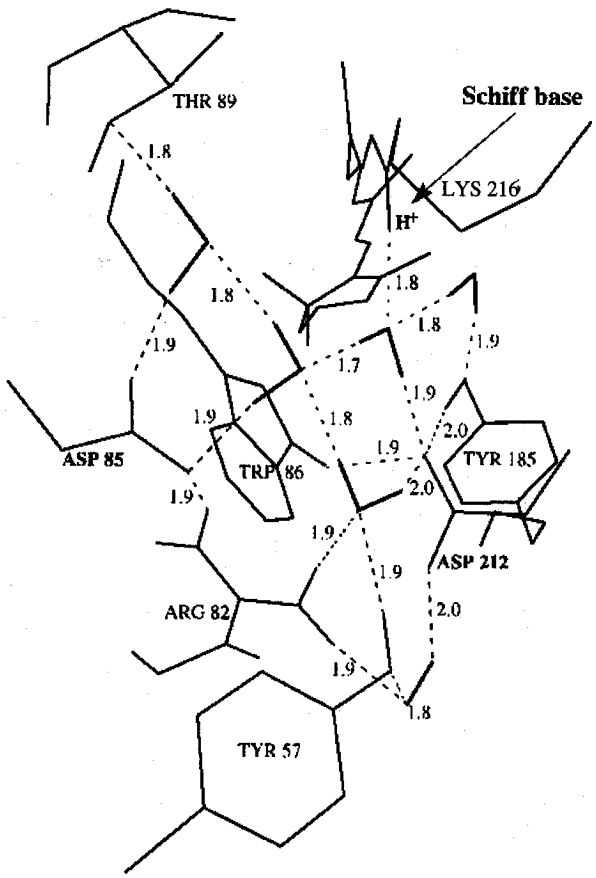

Fig. 3. Structural features of the refined bacteriorhodopsin binding site.

Evaluation of pK_a *Values*

Calculations of the pK_a values for the ionizable groups in bR have been carried out by Bashford and Gerwert,[39] and by Sampogna and Honig.[40] Both studies used finite difference methods for the solution of the Poisson–Boltzmann equation to determine the electrostatic potential energy of charged groups within the protein interior, using a continuum dielectric model. In Bashford and Gerwert,[39] a model of bR_{568} was considered with a dielectric constant of 4 for the protein interior and the surrounding membrane plane, and a dielectric constant of 80 for the surrounding solvent and interior protein cavities. The calculated titration curves for the Schiff base show complex behavior, suggested to be due to the strong electrostatic coupling between the charged groups in the retinal binding site. This study also found that calculated pK_a values compared more favorably with observed values when Arg-82 was positioned close to Asp-85.

In Sampogna and Honig,[40] a similar electrostatic calculation method was used with a model of bR in both the all-*trans* and the 13-*cis* configurations. The calculations also considered the case that Arg-82 is positioned as in the Henderson structure, as well as the case that Arg-82 is oriented towards Asp-85, close enough to form a salt bridge with this group. The results revealed, as in the Bashford and Gerwert study, a complex titration behavior for the Schiff base and for the Asp-85/Asp-212 residues, as well as favorable comparisons with observation when Arg-82 was repositioned near Asp-85. The calculated Schiff base pK_a value dropped by several units and the Asp-85 pK_a increased similarly when retinal was changed from the all-*trans* to the 13-*cis* conformation.

Scharnagl et al.[94] carried out MD and electrostatics calculations to study conformational changes of the protein and retinal as well as the energetics of the proton transfer process up to the M_{412} intermediate of the photocycle. The calculated pairwise electrostatic interactions in the bR ground state (the Henderson structure) gave insight into the individual contributions to pK_a shifts. The L_{550} and M_{412} intermediates were generated by enforcing a 13-*cis* isomerization of the ground-state structure and subsequent proton transfer from the Schiff base to Asp-85. The authors employed a subnanosecond

equilibration at 300 K to cover the millisecond range of the photocycle from bR_{568} to M_{412}, employing a procedure similar to that in ref 79. The complex pH-dependence of the proton release and uptake pattern found for the M_{412} intermediate was studied. The calculations in ref 94 demonstrated also that protein conformational changes in the photocycle of bR shift the acid–base equilibria of retinal and of key residues in the binding site. The authors suggested that the $L_{550} \rightarrow M_{412}$ transition is achieved through a transfer of the Schiff base proton to a nearby bound water molecule and then to Asp-85. The calculation also showed that Arg-82 induces a reduction of the pK_a value of Glu-204, which has been suggested to be the group which releases the pumped proton to the extracellular side.

RECENT MD STUDIES OF bR'S PHOTOCYCLES

The photocycles of bacteriorhodopsin, as shown in Fig. 2, have been studied for over two decades, but still little is known about the functional transformations involved in these cycles. In fact, the proton switch mechanism, invoked to irreversibly transfer the pumped proton between the cytoplasmic channel and the extracellular channel, is attributed, in turn, to motions of the retinal Schiff base[11,18,70,81,82] to overall protein conformational changes[66,80] and, most recently, to a shuttling of Arg-82 between an extracellular and a cytoplasmic orientation.[95]

Photocycle intermediates have been well characterized through kinetic methods, optical, resonance Raman, and infrared spectroscopic methods, mutant studies, and otherwise. These methods have identified essential side groups, protonation states, rough isomeric transformations, and timescales. Unfortunately, the information about the detailed geometry of the protein is extremely limited. As pointed out above, the authors of this review start from the supposition that the proton switch underlying proton pumping in bacteriorhodopsin involves precise sterochemical transformations of the retinal Schiff base which cannot be resolved directly through observation at present, and possibly not for some time.

Theoretical investigations based on quantum chemical calculations of retinal's ground- and excited-state potential surfaces, together with molecular dynamics studies, might point a way out of the dilemma described. Such an approach can incorporate all available information, e.g., regarding the structure of bR, the isomeric states of retinal, and the protonation states of side groups. However, there are several difficulties connected with this approach. Foremost, theoretical methods are inherently imprecise, in particular, for systems as complex as bR. Furthermore, the low-resolution structure of bR_{568} derived from electron microscopy may contain significant errors and does not include any water, which apparently is functionally important. Nevertheless, theoretical investigations can suggest alternatives for the pump mechanism as well as new experiments. Most importantly, such investigations can discern some of the key issues on which the field needs to focus in order to answer the question one day of how the proton pump in bR actually works. An example of such an issue is the role of water in bR. Below we will show what further issues the theoretical investigations have brought forth.

Simulation of the complete photocycles of bR poses considerable difficulties due to the very long (millisecond) timescale involved. The short-lived early intermediates of the bR_{568} photocycle involved in the transitions $bR_{568} \rightarrow J_{625} \rightarrow K_{590} \leftrightarrow L_{550}$ (see Fig. 2a) are amenable to direct calculation. The early stages of the photocycle play a very important role in the photocycle, in that the absorption of a photon and subsequent isomerization of retinal followed by relaxation ($bR_{568} \rightarrow J_{625} \rightarrow K_{590} \leftrightarrow L_{550}$) provide the means by which retinal and the counterion residues are prepared for Schiff base deprotonation and Asp-85 protonation. Our description organizes itself along the indicated timescales of the photocycles. First we describe simulations of the very early step in the photocycle, involving the J_{625} intermediate and leading to the K_{590} intermediate. We then discuss the K_{590} intermediate and its evolution to the L_{550} intermediate. The proton switch step in the photocycle, involving the so-called M_{412} intermediate, is then discussed at length. Finally, we review a study of the photocycle of bR_{548} (see Fig. 2b).

Lack of an Accurate Excited-State Potential

Upon absorption of a photon, ground-state retinal (bR_{568}) undergoes the reaction

$$bR_{568} \rightsquigarrow bR^* \text{ (200 fs)} \xrightarrow{500\text{ fs}} J_{625} \xrightarrow{3\text{ ps}} K_{590}$$

bR* denotes the optically allowed singlet excited state and J_{625} and K_{590} denote the first spectroscopically identifiable intermediates, 200 fs is the apparent lifetime of the excited state bR*, and 500 fs and 3 ps are the rise times of the J_{625} and K_{590} intermediates, respectively. Retinal exists as an all-*trans* isomer in the bR_{568} ground state. The K_{590} state is readily trapped at low temperatures and contains retinal as a 13-*cis* isomer, i.e., the photoreaction of bR_{568} involves an all-*trans* $\rightarrow$ 13-*cis* isomerization.

Obviously, the key determinant for bR's photoreaction, initiating the photocycle, is the excited-state potential energy surface of retinal and its crossings with the

ground-state surface. Despite the ubiquitous occurrence of photoisomerization processes in polyene-type compounds, strikingly little is known about the potential surfaces involved, neither the number of relevant electronic states contributing to the photodynamics nor the shape of the potential surfaces. This situation is compounded by the fact that polyene electron systems pose a formidable challenge to quantum chemistry due to the highly correlated nature of the involved electronic states, which requires extended multi-electron basis sets for suitable descriptions.[58]

Until recently, no quantum chemical method could reliably determine excited-state potential surfaces for electron systems of the size found in retinal. Using the program MOLPRO,[96,97] we have recently achieved the evaluation of the excited-state potential surfaces governing photoisomerization processes for retinal analogues in vacuo; we are presently extending these calculations to include the local electric fields at the retinal binding site in bR_{568}. A potential surface governing the torsion of retinal around the C_{13}–C_{14} bond is presented in Fig. 4. The potential surface provided is actually for the corresponding bond of the retinal analogue $[CH_2\text{-}(CH)_3\text{-}(C_2H_3)\text{-}(CH)_2\text{-}NH\text{-}CH_3]^+$. The figure shows the torsional angle dependence of the energies of the ground state (S_0), of the first excited state (S_1), and of the second excited state (S_2). A simple interpretation of the corresponding electronic states is supplied in Fig. 4: S_0 contains two π-electrons in the bonding orbital, S_1 contains one π-electron in the bonding and one in the anti-bonding orbital, and S_2 contains two π-electrons in the anti-bonding orbital. State S_1 is strongly optically allowed from the ground state, i.e., absorption of a photon populates mainly this state. State S_2 is strongly two-photon allowed (for an overview on the behavior of polyene excited states, see ref 58) and is responsible for the two-photon absorption reported in ref 98; state S_2 has already been described for an octatetraene-type retinal Schiff base analogue in ref 11. Upon torsion around the C_{13}–C_{14} bond, the state S_2 lowers its energy to become the ground state for the 13-*cis* geometry, while the ground state S_0 becomes the second excited state; this behavior is indicated through dashed lines in Fig. 4. State S_1 remains the first excited state upon torsion, exhibiting an energy barrier at the 90° geometry; this feature is indicated again through a dashed line. The numerically evaluated surface follows surprisingly closely the stated approximate (see dashed lines) behavior.

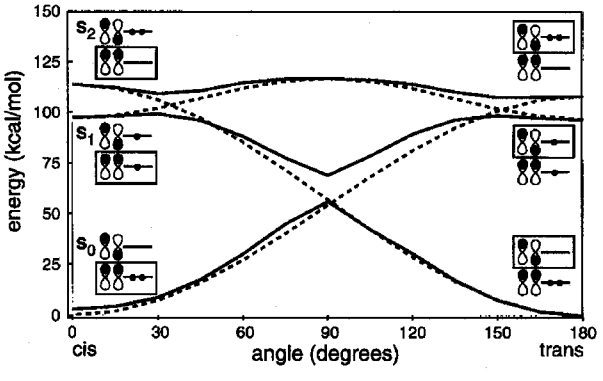

Fig. 4. Ground-state and excited-state potentials of $[H_2C{=}(CH){-}(CH){=}(CH){-}(CH_3{-}C^*){=}(C^*H){-}(CH){=}NH^+{-}CH_3]$, an analogue of the protonated Schiff base of retinal. The dependence of the energies of the ground (S_0) and of the first as well as the second excited state (S_1, S_2) on the torsional angle of the bond C*=C* is shown. The indicated bond corresponds to the C_{13}–C_{14} bond of retinal in bR. Dashed lines sketch potentials thought to represent the electron configurations of the two π-electrons involved in the C*=C* bond. The square box identifies the corresponding electron configurations of the *trans* and *cis* geometries; torsion by 180° alters a bonding π-orbital into an anti-bonding π-orbital and vice versa.

The potential surfaces in Fig. 4 suggest the following excited-state dynamics: upon light absorption, retinal is promoted from state S_0 to state S_1; retinal then begins to rotate around its C_{13}–C_{14} bond on a relatively flat S_1 potential surface until state S_1 crosses state S_2; at this point the surface curves down in energy towards a minimum at 90°. At this point retinal has a chance to remain on the dashed potential (see Fig. 4), continuing the energetically downhill motion to reach the 13-*cis* geometry.

A sensible approach for simulation of the photoisomerization described is to employ model potential surfaces in molecular dynamics simulations. In fact, the photoisomerization reaction was described in Humphrey et al.[65] in three steps governed by three potential surfaces: during the initial excited-state dynamics a potential along the C_{13}–C_{14} and C_{14}–C_{15} dihedral angles was used, which modeled the S_1 state with maxima at the all-*trans* and 13-*cis* geometries and with a minimum at the 90° geometry. The subsequent excited-state → ground-state surface crossing event was described through a potential surface with a single maximum at the all-*trans* geometry, modeling a continuous surface in the ground- and excited-state crossing region identical to (2) and following the corresponding dashed line in Fig. 4. The concluding ground-state relaxation was governed by the ground-state (S_0) potential surface.

The simulations of the photoisomerization of bR_{568} in ref 65 followed those in ref 79 in that two types of photoisomerization potentials were employed: one, referred to as the 13-*cis* model potential, assumes a barrier of 10 kcal/mol for rotation around the C_{14}–C_{15} single bond

in the S_1 state; the other, referred to as the 13,14-di*cis* model potential, assumed a barrier of only 1 kcal/mol for this rotation.

The J_{625} Intermediate

Due to its short lifetime, the J_{625} state is more elusive than the K_{590} state. J_{625}, with an observed quantum yield of 0.64 ± 0.04,[99-101] starts to appear at about 200 fs when the excited state bR* begins to decay. J_{625} has a lifetime of 500 fs as observed through its absorption spectrum before the appearance of the K_{590} absorption. Raman spectroscopy suggests that the J_{625} state is a vibrationally excited form of K_{590} which thermally decays in 3 ps to its vibrational ground state, i.e., to K_{590}.[102] This interpretation of J_{625} concurs with femtosecond pump-probe experiments.[102-105] As a result of these studies, a one-dimensional model had been proposed[102,104] which attempted to describe the photodynamics of retinal: upon absorption of a photon, the electronically excited retinal moves coherently along the excited state (bR*) potential-energy surface, crossing nonadiabatically in 200 fs to the ground state, where it remains vibrationally "hot" for 500 fs and then decays either back to the initial state bR_{568} or, within 3 ps, to the product state K_{590}. This model does not explicitly include the protein in the reaction coordinate; MD simulations indicate that the protein actually plays a key role.

The nature of the J_{625} intermediate, naturally, is one of the first issues to address in studying the photocycle of bR by means of MD simulations. A revelation about the nature of this state is provided by the observation that a J-like state arises even in the case that bR is reconstituted with a retinal analogue which is incapable of an all-*trans* → 13-*cis* isomerization.[106] This implies that a description of the spectral shift experienced by retinal after photoexcitation of bR_{568} requires neither knowledge of the excited-state potential surface nor an exact description of the photoisomerization reaction. One may also surmise that the decay of the J_{625} state is not due to an underlying geometrical relaxation process. In fact, the molecular dynamics study in ref 107 revealed an alternative explanation of the J_{625} state: the spectral shift 568 nm → 625 nm reflects the polarization of the protein matrix induced by the strong change of dipole moment of retinal when the latter is electronically excited. The molecular dynamics simulation in ref 107 assumed that retinal is promoted to the excited state and then returns to the ground state after 200 fs. The simulation, which accounted for the excited state through its altered charge distribution, yielded a strong polarization of the protein matrix with a maximum at about 500 fs. This polarization results in a red shift of the spectrum of retinal. The simulation also revealed that the electronic excitation energy which, in this description, was liberated into the retinal nuclear degrees of freedom via torsion of its C_{13}–C_{14} bond, relaxes into the protein matrix on a timescale of 3 ps, suggesting that the decay of the J_{625} intermediate in the photocycle reflects the vibrational cooling of retinal.

The K_{590} and L_{550} Intermediates

While the simulations of the photocycle of bR_{568} in ref 79 followed the motion of a single trajectory of bR during the entire photocycle, a more detailed study of just the early intermediates by Humphrey et al.[65] modeled the initial steps of the photocycle for a sample of fifty trajectories. In this study, both the 13-*cis* and 13,14-di*cis* photoisomerization models were simulated, using for the initial equilibrium configuration of bR_{568} the refined, all-atom structure in ref 83. For each model, instead of a single trajectory, fifty separate 5-ps simulations were performed for the $bR_{568} \rightarrow J_{625} \rightarrow K_{590}$ photoisomerization process, each trial distinguished by different initial atomic velocities. The multiple trials accounted for a possible heterogenity in the photodynamics and subsequent isomerization products (K_{590}). The photoisomerization reaction was described in ref 65 in three steps governed by three potential surfaces as described above (see Fig. 4): the surface of the excited state S_1, an intersystem crossing potential (dashed lines in Fig. 4), and the surface of the ground state S_0.

From the separate 5-ps trials emerged fifty K_{590} photoproducts, which could be classified according to their geometry into four classes, distinguished by the orientation of the N–H$^+$ Schiff base bond: a class with the N–H$^+$ pointing "up", i.e., toward the cytoplasmic side of bR (case 1), corresponding closely to a pure 13-*cis*-retinal geometry; a class with the N–H$^+$ pointing roughly perpendicular to the membrane normal (case 2), corresponding to a 13-*cis*-retinal with strong single bond torsions; a class with the the N–H$^+$ pointing "down", i.e., toward the extracellular side of bR with retinal in a pure a 13,14-di*cis* conformation (case 3); and, finally, a class retinal remaining in its initial all-*trans* geometry, having failed to complete the isomerization process (case 4). As a measure of the N–H$^+$ orientation, θ_{SB} was defined as the angle between a line formed by N–H$^+$ and a line connecting the Schiff base nitrogen and the Asp-96 carboxyl. For small θ_{SB}, N–H$^+$ points toward Asp-96, while for θ_{SB} close to 180° the orientation of N–H$^+$ is toward the extracellular side of the protein. Table 1 summarizes the definitions of these cases, and lists the percentage of each case present in the simulations.

The structures summarized in Table 1 constitute the simulated K_{590} intermediate. For the 13-*cis* model, all trials isomerized completely within the first 500 fs, which is the experimentally measured time for the formation of J_{625}. The question arises, which case corre-

Table 1. Definitions of four classes (cases) of retinal geometries used to categorize isomerization trials, and percentage of cases present in each set of simulations

Case	Definition	300 K		77 K	
		13-*cis*	13,14-di*cis*	13-*cis*	13,14-di*cis*
1	13-*cis*, $\theta_{SB} \leq 60°$	58	12	72	0
2	13-*cis*, $\theta_{SB} > 60°$	36	2	0	0
3	13,14-di*cis*, $\theta_{SB} > 90°$	6	28	28	76
4	all-*trans*, $\theta_{SB} > 90°$	0	50	0	22

sponds to the initial state of bR's pump cycle? The case 1 structures, while the most frequently occurring products for the 13-*cis* model potential, assume an orientation of the Schiff base N–H$^+$ which is unsuitable for transfer of the Schiff base proton to Asp-85; instead, the orientation would be suitable for pumping the proton in the direction opposite to that observed under physiological conditions. The case 2 and case 3 structures, however, both provide a direct pathway for proton transfer: the N-H$^+$ bond is oriented such that the Schiff base proton is readily transfered to Asp-85. Case 2 in particular provides a compelling candidate for the actual pump cycle: in this case, the Schiff base forms a hydrogen bond with a water molecule directly hydrogen-bonded to Asp-85 (water W_C in Fig. 5), which can act as an intermediate in the transfer process; the hydrogen bond between the Schiff base and water stabilizes retinal in a geometry with the N–H$^+$ group oriented perpendicular to the membrane normal; transfer of the Schiff base proton to Asp-85 would abolish the attraction between the Schiff base and W_C and would allow retinal to complete its all-*trans* → 13-*cis* isomerization such that the Schiff base nitrogen would eventually point into an orientation in which it can accept a proton from Asp-96.

It is interesting to speculate about the relevance of the photoproducts of cases 1–4 for the actual bR_{568} photocycle. The emergence of the case 4 geometry, in which retinal remains in an all-*trans* geometry, corresponds to a quantum yield of less than one for the photoisomerization (the actual quantum yield measures 0.64 ± 0.04, as observed in refs 99–101). The emergence of case 3 photoproducts with a 13,14-di*cis* geometry depends on the character of the excited-state potential surface of retinal in bR_{568}: if this surface entails a significant barrier which hinders the co-rotation around the C_{14}–C_{15} bond of retinal during the all-*trans* → 13-*cis* isomerization then this product will not arise. Lack of knowledge of the excited-state potential deprives one of a conclusion in this regard, except to state that case 3 products may actually be prevented by the nature of the excited state surface. However, whatever this surface, the production of both case 1 (pure 13-*cis*) and case 2 geometries (13-*cis* with strong torsions around retinal's single bonds) appears to correspond to a genuine outcome of bR_{568}'s photoreaction. This implies that bR_{568} would engage in at least two photocycles, one starting from the case 2 product, probably the functional cycle, and one starting from the case 1 (N_{520}-type, however, in an unrelaxed protein matrix) product, probably an idle cycle. Heterogeneous photocycles have been suggested by the observations in refs 26,108,109; ref 109 suggests, in particular, that a cycle that bypasses the M_{412} intermediate arises, a behavior to which a cycle starting from a case 1 retinal geometry would conform.

The results in Table 1 suggest that the ratio of case 1 to case 2 photoproducts is altered upon cooling; in fact, at 77 K only case 1 photoproducts arise for a 13-*cis* model potential. This behavior might explain why the pump cycle of bR_{568}, at 77 K, is trapped at the K_{590} intermediate: the path to case 2 photoproducts might be blocked at low temperature such that only case 1 photoproducts develop. However, the case 1 photoproducts cannot continue the pump cycle since they do not bear a proton pathway from retinal to Asp-85. Indeed, upon warming of bR after formation of the K_{590} intermediate at 77 K, an M_{412} intermediate is not observed.[110]

To simulate formation of the L_{550} intermediate, the study in ref 65 employed the method of simulated annealing to span the $K_{590} \leftrightarrow L_{550}$ transition which requires about 2 μs. Since annealing calculations are time consuming, only a single case 2 structure could be investigated for the 13-*cis* model, and a single case 3 structure for the 13,14-di*cis* model. The resulting L_{550} structure showed for both models relatively little deviation from the original K_{590} structure. An important result is that the L_{550} structure for the 13-*cis* model maintained the hydrogen bond between the Schiff base and water W_C, supporting the suggested proton transfer mechanism. This L_{550} structure involved a twisted and strained retinal, the geometry of which is in agreement with observations by means of polarized FTIR spectroscopy.[111]

The three important outcomes of the MD studies in ref 65 were (1) the participation of water in the early stages of the proton pump cycle; (2) the emergence of

several photoproducts for bR_{568}, namely, besides an unisomerized retinal (case 4), three 13-*cis*-retinals (cases 1–3 above) with possibly separate photocycles; and (3) the identification of the case 2 structure of retinal as the most likely structure of the K_{590} and L_{550} intermediates. Figure 5 summarizes the most likely structural transformations of bR_{568}'s photocycle accompanying the K_{590} and L_{550} intermediates.[65] The simulations emphasize the requirement for an accurate experimental determination of the position of water molecules in the retinal binding site, and the need for a better (i.e., accurate quantum chemical) description of the excited state potential energy surface of retinal.

The M_{412} Intermediate

The M_{412} intermediate is formed in bR_{568}'s photocycle after transferring the proton from retinal's Schiff base in the L_{550} intermediate to Asp-85, which in turn is connected to the extracellular side of bR. The M_{412} intermediate is terminated through transfer of a proton from Asp-96, which in turn receives a proton from the cytoplasmic side of bR. The M_{412} intermediate, accordingly, embodies the proton switch between the proton release pathway and the proton uptake pathway of bR,[14,75,112,113] the switch disconnecting retinal from the extracellular side and connecting it to the cytoplasmic side.[18,114–116] The M_{412} intermediate has been described[117] by means of MD simulations.

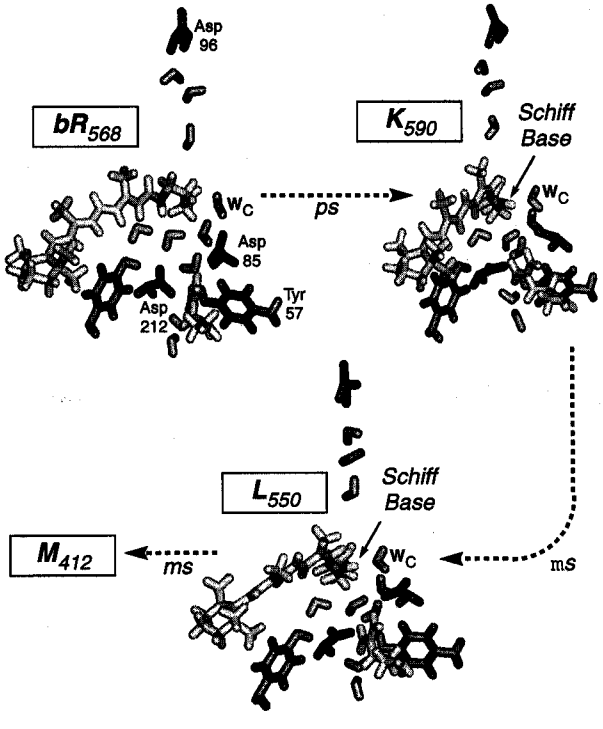

Fig. 5. Suggested structures of early intermediates in the bacteriorhodopsin photocycle, $bR_{568} \rightarrow J_{625} \rightarrow K_{590} \rightarrow L_{550}$.

Formation and decay of the M_{412} intermediate occurs on microsecond and millisecond timescales, respectively; at present, computational resources allow one to cover time periods of at most a few nanoseconds in MD simulations. The descriptions of the M_{412} intermediate in ref 117 resorted, therefore, to simulated annealing,[118] which also had been employed[65] to reach the L_{550} intermediate. The simulations in ref 117 considered both the 13-*cis* and 13,14-di*cis* model, using as starting points corresponding L_{550} structures as simulated in ref 65. Summarized here are the results of simulations of the M_{412} state starting from the case 2 structure of the bR_{568} photoproduct as shown in Fig. 5, e.g., for the 13-*cis* model.

The resulting simulations yielded a heterogeneous M_{412} intermediate which actually constitutes a reaction process of several successive protein conformations and retinal geometries. Experiments indeed revealed that there are at least two components to the M_{412} intermediate,[119,120] a third component being suggested recently as well.[121] The configuration of waters, amino acid side groups, and hydrogen bonds during the early stage of the simulated M_{412} intermediate are presented in Fig. 6a. In the counterion region, three water molecules (F, G, and I) arrange themselves to connect to the hydroxyl group of Tyr-57 and to the oxygen of the Thr-89 hydroxyl moiety. These waters are nearly coplanar and form a hydrogen bond complex with their hydroxyl groups oriented approximately along a straight line. The hydroxyl group of Asp-85 lies almost perpendicular to the water plane. The distance between the hydrogen of the hydroxyl group in Asp-85 and its closest possible hydrogen-bonding acceptor, the oxygen of water G, is 2.44 Å. Both oxygens of the Asp-85 carboxylate do not have a close donor to form strong hydrogen bonding and, as a result, Asp-85 does not interact with the water chain F, G, and H. This result is consistent with FTIR measurements which indicate that Asp-85 is in a hydrophobic environment at the M stage.[122] The lack of hydrogen bonding between water and Asp-85 can explain the prevention of a back-transfer of the proton from Asp-85 to retinal.

During the early stage of the M_{412} intermediate, as simulated in ref 117, significant protein conformational changes developed, in particular, a 60° bend of helix F (see Fig. 1a) in a direction away from the center of bR. This bend was localized around Arg-175, Asn-176, and Val-177, as shown in Fig. 7. The simulated protein conformational state appears to be in agreement with the observations reported in refs 123, 124. Concomitant with the bend of helix F, the ring of Tyr-185, on the extracellular side of helix F, moved by about 3.8 Å away from the Schiff base towards the extracellular side and

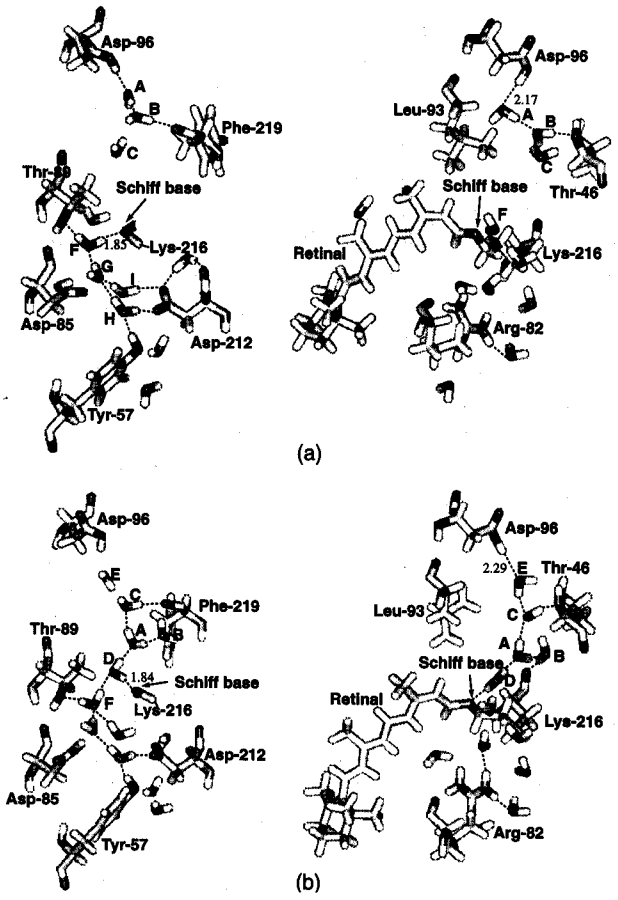

Fig. 6. Solid model images of (a) early M_{412} and (b) late M_{412}, in the vicinity of the Schiff base, from two different perspectives. Dashed lines between atoms represent hydrogen bonds.

towards the ring region of retinal, as shown in Fig. 7. This significant motion is due to a weakening of the interaction of Tyr-185 with the hydrogen bond network of waters F, G, I, and H through proton transfer from retinal to Asp-85.

The bend of helix F, as described in ref 117, opens the cytoplasmic channel of bR and allows access of further waters. Accordingly,[117] two water molecules, D and E, were placed as shown in Fig. 6b, in the cytoplasmic channel. Water D moved towards the retinal Schiff base nitrogen which then rotated towards the cytoplasmic direction to hydrogen-bond to this water. The rotation led to a breaking of the hydrogen bond between the retinal Schiff base, and water F. The hydroxyl group of water F hydrogen-bonded with water D, connecting, thus, the cytoplasmic channel and the counterion region at this point. This rearrangement induced, during the late stage of the M_{412} intermediate, a hydrogen bond network between Asp-96, Thr-46, Phe-219, Lys-216, the retinal Schiff base and waters E, F, G, I, and H; this network, presented in Fig. 6b, is optimal for proton transfer from Asp-96 to retinal. An analysis of the simulations revealed that the water molecules during the late stage of M_{412} are less mobile than during the early stages of M_{412}, corresponding to a significantly reduced energy and entropy, in agreement with the observations in refs 115,125. A comparision of the retinal geometries and hydrogen bond networks of the L_{550} intermediate in Fig. 5 and of the early and late stages of M_{412} in Fig. 6 shows how bR may act as a proton switch, disconnecting a hydrogen bond network between retinal and Asp-85 and establishing a network between retinal and Asp-96. The simulations in refs 65 and 117, thus, identified and made evident the protein switch function of the M_{412} intermediate.

bR_{548} and its Photocycle

Bacteriorhodopsin converts in the dark within about 30 min to a dark-adapted state assuming a 1:2 equilibrium between the bR_{568} and the bR_{548} forms,[17] the latter containing retinal in a 13-*cis*,15-*syn* geometry.[19–21] This conversion contrasts with the behavior of retinal in solution where an all-*trans* configuration is more stable.[126] Obviously, the retinal binding site of bR stabilizes the 13-*cis*,15-*syn* geometry of bR_{548}. The structure of dark-adapted bR, i.e., of bR_{548}, and its photocycle have been studied.[54] The stabilization of a 13-*cis*,15-*syn* retinal geometry appears to be consistent with the structure of bR_{548} obtained in ref 54 and presented in Fig. 8. This structure suggests that for bR_{548}, the distances between the Schiff base proton and the most proximate oxygens of Asp-85 and Asp-212 measure 4.6 Å and 4.2 Å, respectively, whereas in the simulations of bR_{568}[83] these distances measured 6.0 Å and 4.6 Å, respectively (Fig. 3). The more proximate position of the negatively-

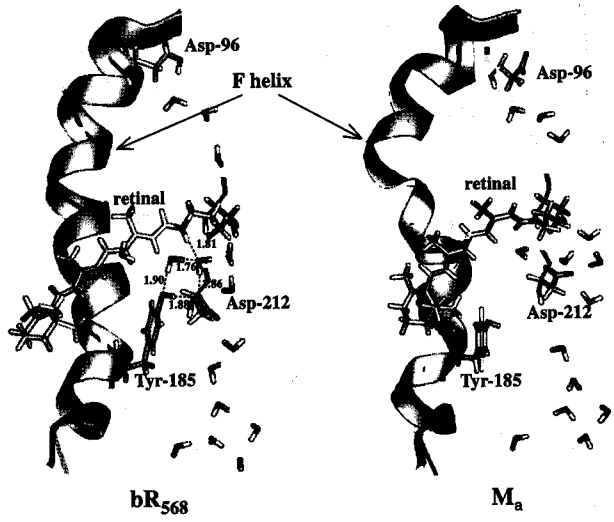

Fig. 7. F helix conformation and its environment in bR_{568} and early M_{412}. Dashed lines between atoms represent hydrogen bonds.

charged aspartic acids to the positively-charged retinal Schiff base stabilizes bR_{548} as compared to bR_{568} and can explain also the blue-shifted spectrum of bR_{548} relative to that of bR_{568}. Spectral (NMR, vibrational, electronic) differences between bR_{568} and bR_{548} were ascribed previously to a twist of the C_{14}–C_{15} bond.[68,127–129] However, such torsion is not seen in the structure in Fig. 8. The simulations in ref 54 attribute the observed differences between bR_{548} and bR_{568} also to steric interactions between C_{14}-H and C_{ε}-H_2 of Lys-216, an explanation which agrees with experiments in which bacterio-opsin is reconstituted with various analogues of 13-*cis*-retinal.[93]

When bR_{548} absorbs a photon, it enters the photocycle shown in Fig. 2b. Spectroscopic measurements detected two early intermediates, J and K_{590}, which form and decay on different timescales;[130] at present, experiments have not yet characterized these intermediates conclusively. Logunov et al.[54] simulated the photoisomerization of the bR_{548} photocycle, initiating the event by instantaneously changing the torsional potential of the C_{13}–C_{14} bond in the same manner as in ref 79. The simulated bR structure reached after 0.6 ps an unstable J-type intermediate with a large torsion around the C_{13}–C_{14} bond and not engaging in hydrogen bonding to side groups or waters. The intermediate was found to relax, through a 30° rotation around the C_{13}–C_{14} bond, to a metastable structure, shown in Fig. 8, assigned to the K_{590} intermediate.

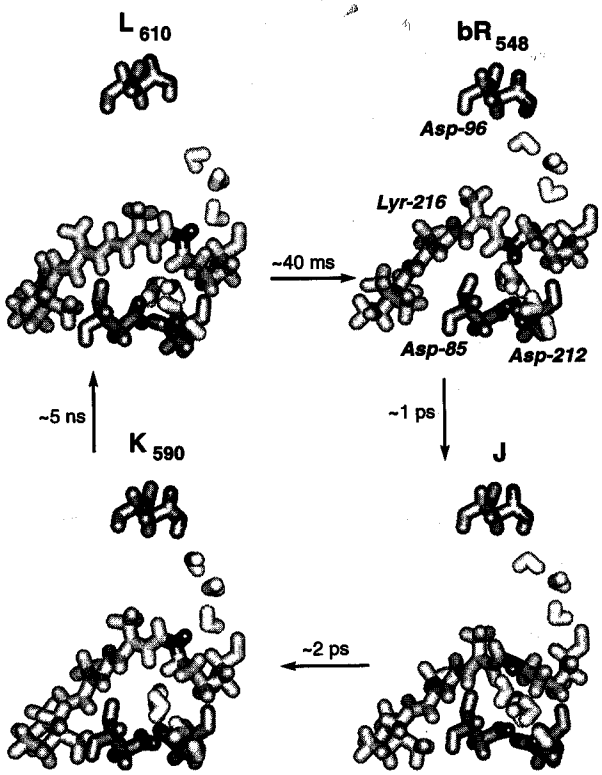

Fig. 8. Intermediates of the photocycle of bR_{548}. Shown are retinal bound to Lys-216, three aspartic acids which play important roles in the photocycle, and water molecules in the binding site.

Application of an annealing scheme, as applied also to the bR_{568} photocycle,[65] led to a third structure, presented also in Fig. 8, which had been assigned to the L_{610} intermediate. A key result of the simulation in ref 54 is that the Schiff base proton of this putative L_{610} intermediate points towards the cytoplasmic side and, thereby, loses its ability to protonate Asp-85. This orientation arises even when one employs a photoisomerization potential of the all-*trans* → 13,14-di*cis* type, as in ref 79. Observations show indeed that retinal does not become deprotonated in the bR_{548} photocycle, i.e., an M_{412} intermediate is not formed. Instead of passing through an unprotonated intermediate, the bR_{548} photocycle decays from a K_{590} and subsequent L_{550} intermediate directly back to bR_{548} with a half-life of 40 ms.[131,132] This behavior suggests that the bR_{548} photocycle does not pump protons. However, an M_{412} intermediate is observed in the photocycle of bR_{548} at pH values higher than 9[133] and for an artificial pigment derived from 13-demethyl,14-F-retinal[134] but proton pump activity had not been studied for these cases. The simulations in ref 54 suggest that the key difference between the bR_{568} and bR_{548} photocycles is the orientation of retinal's Schiff base proton in the L_{550} intermediate; an L_{550} intermediate with a pure 13-*cis* geometry does not yield an M_{412} intermediate and, hence, does not lead to proton pumping under normal conditions. One may speculate that such an intermediate, when it becomes deprotonated, actually releases the Schiff base proton to the cytoplasmic side. Indeed, recent simulations of a D85N mutant of bacteriorhodopsin have shown that the replacement of Asp-85 by asparagine also has the effect of leading to a pure 13-*cis* type L_{550} intermediate. In this case it is of interest that the mutant, in the presence of yellow light, yields a proton pump in which the pump direction is reversed.[135]

It has been observed that following light absorption, about 10% of the isomerized bR_{548} experiences an isomerization around two bonds, producing an all-*trans*, 15-*syn* isomer.[50] A number of pathways have been proposed for the light adaptation, with various steps of the 13-*cis* photocycle as possible branching points.[51,131,136–139] It is conventionally assumed that the leakage occurs during the post-K stages of the bR_{548} cycle through a 15-*syn* → 15-*anti* isomerization leading directly to bR_{568}. Some experimental data indicate that the bR_{548} photocycle converts to the bR_{568} photocycle early in the excited state.[50–53] The simulations of the primary photoisomerization process in ref 54 have shed light also on the question how the photocycle of bR_{548} "leaks"

into the photocycle of bR_{568}. In fact, the simulations suggest that the leakage pathway involves the occurence of a 13-*cis*,15-*syn* → all-*trans*,15-*anti* photoisomerization: 70% of the simulated photoreactions produce J and K_{590} states as shown in Fig. 8; 30% of the simulated photoreactions engaged in a 13-*cis*,15-*syn* → all-*trans*,15-*anti* isomerization. We note that simulations of the bR_{568} photocycle did not produce any co-isomerization of the C=N bond. The possibility of a photoisomerization around two double bonds induced by a single photon absorption has been demonstrated experimentally in visual pigment isomerization.[140]

FUTURE MD STUDIES AND CHALLENGES

The most essential outcome of the MD studies of bR reported[54,65,83,107,117] has been the demonstration of a potentially critical role of water and of minute reorientations of retinal's Schiff base nitrogen in controlling proton pumping in bR_{568}. The results exemplify the important role of MD simulations in extending investigations on bR to a level of detail which often is beyond experimental resolution, but which is crucial for an understanding of enzyme mechanisms. MD simulations are intrinsically inaccurate and their results must be verified eventually through observations, but such simulations provide compelling suggestions for further experimental and theoretical investigations from which research on bR may benefit immensely. We conclude this review, therefore, with suggestions of MD studies with a high potential to advance our knowledge of bR.

Refinement of bR and Water Placement

One of the major tasks in the field of bR modeling is the generation of reliable, highly-refined structural models of the protein. A number of existing structures of bR and its photointermediates need to be compared on a quantitative basis in order to make the best choice among them. A crucial issue is the accurate placement of water molecules inside bR, which is believed to play an important structural and functional role, and is incorporated in almost all current bR models.[83,95,141] Unfortunately, there still exists a high degree of arbitrariness in the placement of water molecules. Some attempts have already been made to place water molecules in the bR binding site based on calculations of the change in free energy in the process of water transfer from bulk to the protein interior.[142] These types of calculations need to be extended to establish a convergence of the predictions made by the researchers.

Need of Ensemble Averages

An essential task is the description of the photocycles of bR, not in terms of one particular MD trajectory, but rather in terms of an ensemble of such trajectories describing variations in bR_{568}'s photoexcitation response. A first step in this direction has already been taken[54,65,117] by modeling multiple initial photoisomerization events for an ensemble of structures taken from a single MD trajectory. However, more extended ensembles, which incorporate structures that are not linked by a single picosecond MD trajectory, are needed.

Use of Long-time Integration Methods

As was pointed out earlier, conventional molecular dynamics techniques cannot cover the complete bR photocycle. To model processes which occur on a long timescale (i.e., longer than 1 ns), one has to employ long-time integration methods. One such technique, simulated annealing, has been applied to describe the L_{550} and M_{412} intermediates.[54,65,117] However, in simulated annealing the timescale is forfeited. Alternative approaches to the problem of long-time dynamics have been suggested.[143–147] A promising avenue is the slow mode integration technique, in which slow modes of a protein are identified and thereafter employed for predicting the long-time conformational changes.[148,149] Another possible alternative for treating the long-time integration problem for the study of bR's pump cycle is to use implicit integrators for the Newtonian equations of motion, which would efficiently damp the short-time fluctuations of a protein (see, e.g., refs 50, 151). One may also employ the method of dihedral angle dynamics, in which all protein degrees of freedom are kept constant except the dihedral angles which are described in the limit of strong friction;[152] however, the increase of the integration time step to 1 ps, suggested in ref 152, is grossly overestimated for densely packed proteins with stiff short-range van der Waals interactions.

Combination of Quantum Chemical and MD Descriptions

Another major challenge is the quantitative prediction of the experimentally observed spectral properties and photoreactivity of bR. This requires a combination of quantum chemical and MD calculations. Many efforts are being put into merging the MD and quantum chemistry techniques.[153–160] A combination of quantum chemistry and MD techniques has been applied to the study of the spectral properties and isomerization potential of in situ retinal.[62,161] The calculations have been able to describe satisfactorily the spectral properties of bR,[161] as well as the thermally activated isomerization of in situ retinal responsible for the dark adaptation of bR.[62] This accomplishment paves a road towards further simulation of the whole bR photocycle by means of combined quantum/classical techniques. However, im-

provements in both the level of quantum chemical ab initio calculations and the accuracy of bR models are needed in order to describe quantitatively the wide range of experimentally observed bR properties.

Quantum/Classical Simulations of Retinal's Photoreaction

The most fascinating process associated with the bR proton pump activity is the primary photoisomerization reaction. It occurs on a timescale of a few hundred femtoseconds and constitutes the fastest chemical process known in biology. The primary photochemical event is not only typical for bR, but is shared by all proteins incorporating the retinal prosthetic group. In situ photoisomerization of retinal is quite different from that in solution in the sense that the arrangement of the protein side groups determines both the stereochemistry and the timescale of the primary photochemical event. It is the primary photochemical event in bR which calls for both a high level of ab initio theory and an accurate representation of the bR active site. A first result of calculations of this type is presented in Fig. 4. The potential surfaces in Fig. 4, describing three electronic states of retinal, can be employed in a quantum/classical mechanical calculation to describe the crossing between the excited-state and ground-state surfaces during photoisomerization.[155,162]

Proton Transfer Reaction

The overall proton pump activity of bR results from a series of elementary proton transfer processes performed mainly in the same vectorial direction from inside to outside of the cell. It is important to understand on a quantitative level the major driving forces, i.e., pK_a values, which determine the rates of the individual proton transfer steps. The problem of adequate modeling of in situ proton transfer reactions extends far beyond the bR proton pump cycle itself, since it is one of the most common elementary chemical processes to be found in a living cell (see, e.g., refs 10,163). The proper description of proton transfer reactions will require, in particular, faithful descriptions of electrostatic forces in bR.

Modeling of Other Retinal Proteins

Finally, expertise accumulated in modeling of bR should be utilized in the study of the closely related retinal proteins halorhodopsin (hR), sensory rhodopsin (sR), and the visual pigments. These proteins bear not only structural similarity (transmembrane seven-helix proteins with a retinal prosthetic group), but also share similar functional characteristics, in particular, an initial photoisomerization event. The major difficulty in modeling the retinal proteins is that their structure has not been resolved experimentally with sufficient accuracy (except for the structure of hR which has been resolved recently by Henderson and coworkers with an accuracy close to that of bR).[164] However, there exists a number of well-developed structural prediction methods which can generate secondary and tertiary structures of proteins with reasonable accuracy.[165] A combination of these methods with the large bulk of experimental data available for retinal proteins could provide a prediction for their structures on which molecular dynamics simulations might be based.

Acknowledgments. The authors wish to thank H.-J. Werner for a collaboration on quantum chemical studies of retinal potential surfaces, from which Fig. 4 resulted, and for hospitality extended to I.L. The research was carried out at the Resource for Concurrent Biological Computing at the University of Illinois, funded by the National Institutes of Health (P41RR05969), the National Science Foundation (BIR-9318159), and the Roy J. Carver Charitable Trust. The majority of simulations were done using Silicon Graphics and Hewlett-Packard workstations operated by the Resource.

REFERENCES AND NOTES

(1) Khorana, H.G. *J. Biol. Chem.* 1988, **263**: 7439.
(2) Birge, R.R. *Annu. Rev. Phys. Chem.* 1990, **41**: 683.
(3) Birge, R.R. *Biochim. Biophys. Acta* 1990, **1016**: 293.
(4) Mathies, R.A.; Lin, S.W.; Ames, J.B.; Pollard, W.T. *Annu. Rev. Biochem. Bioeng.* 1991, **20**: 491.
(5) Lanyi, J.K. *J. Bioenerg. Biomembr.* 1992, **24**: 169.
(6) Oesterhelt, D.; Tittor, J.; Bamberg, E. *J. Bioenerg. Biomembr.* 1992, **24**: 181.
(7) Ebrey, T. In *Thermodynamics of Membranes, Receptors and Channels*; Jacobson, M., Ed.; CRC Press: New York, 1993, p. 353.
(8) Henderson, R.; Unwin, P.N.T. *Nature* 1975, **257**: 28.
(9) Henderson, R.; Baldwin, J.M.; Ceska, T.A.; Zemlin, F.; Beckmann, E.; Downing, K.H. *J. Mol. Biol.* 1990, **213**: 899.
(10) Lanyi, J. *Nature* 1995, **375**: 461.
(11) Schulten, K.; Tavan, P. *Nature* 1978, **272**: 85.
(12) Mogi, T.; Stern, L.J.; Chao, B.H., Khorana, H.G. *J. Biol. Chem.* 1989, **264**: 4192.
(13) Mogi, T.; Marti, T.; Khorana, H.G. *J. Biol. Chem.* 1989, **264**: 14197
(14) Braiman, M.S.; Mogi, T.; Marti, T.; Stern, L.J.; Khorana, H.G., Rothschild, K.J. *Biochemistry* 1988, **27**: 8516.
(15) Stern, L.J.; Khorana, H.G. *J. Biol. Chem.* 1989, **264**: 14202.
(16) Gerwert, K.; Hess, B.; Soppa, J.; Oesterhelt, D. *Proc. Natl. Acad. Sci. USA* 1989, **86**: 4943.
(17) Ohno, K.; Takeuchi, Y.; Yoshida, M. *Biochim. Biophys. Acta* 1977, **462**: 75.
(18) Orlandi, G.; Schulten, K. *Chem. Phys. Lett.* 1979, **64**: 370.

(19) Harbison, G.; Smith, O.; Pardoen, J.; Winkel, C.; Lugtenburg, J.; Herzfeld, J.; Mathies, R.; Griffin, R. *Proc. Natl. Acad. Sci. USA* 1984, **81**: 1706.
(20) Smith, S.; Myers, A.; Pardoen, J.; Winkel, C.; Mulder, P.; Lugtenburg, J.; Mathies, R. *Biophysics* 1984, **81**: 2055.
(21) Livnah, N.; Sheves, M. *J. Am. Chem. Soc.* 1993, **115**: 351.
(22) Lozier, R.H.; Bogomolni, R.A.; Stoeckenius, W. *Biophys. J.* 1975, **15**: 955.
(23) Aton, B.; Doukas, A.G.; Narva, D.; Callender, R.; Dinur, U. *Biophys. J.* 1980, **29**: 79.
(24) Baasov, T.; Friedmann, N.; Sheves, M. *Biochemistry* 1987, **26**: 3210.
(25) Baasov, T.; Sheves, M. *J. Am. Chem. Soc.* 1989, **109**: 1594.
(26) Wu, S.; El-Sayed, M.A. *Biophys. J.* 1991, **60**: 190.
(27) Ulrich, A.S.; Wallat, I.; Heyn, M.P.; Watts, A. In *Structures and Functions of Retinal Proteins*; Rigaud, J.L., Ed.; Colloque INSERM/John Libbey Eurotext Ltd.: Montrouge, France, 1992; Vol. 221, p. 247.
(28) Albeck, A.; Livnah, N.; Gottlieb, H.; Sheves, M. *J. Am. Chem. Soc.* 1992, **114**: 2400.
(29) Trissl, H. *Photochem. Photobiol.* 1990, **51**: 793.
(30) Rath, P.; Krebs, M.P.; He, Y.; Khorana, H.G.; Rothschild, K.J. *Biochemistry* 1993, **32**: 2272.
(31) Balashov, S.P.; Govindjee, R.; Kono, M.; Imasheva, E.; Lukashev, E.; Ebrey, T.G.; Crouch, R.K.; Menick, D.R.; Feng, Y. *Biochemistry* 1993, **32**: 10331.
(32) Ovchinnikov, Y.A.; Abdulaev, N.G.; Feigina, M.Y.; Kiselev, A.V.; Lobanov, N.A. *FEBS Lett.* 1979, **100**: 219.
(33) Khorana, H.G.; Gerber, G.E.; Herlihy, W.C.; Gray, C.P.; Anderegg, R.J. *Proc. Natl. Acad. Sci. USA* 1979, **76**: 5046.
(34) Karplus, M.; McCammon, J.A. *Annu. Rev. Biochem.* 1983, **53**: 263.
(35) Karplus, M.; McCammon, J.A. *Sci. Am.* 1986, **4**: 30.
(36) McCammon, J.A.; Harvey, S.C. *Dynamics of Proteins and Nucleic Acids*; Cambridge University Press: Cambridge, 1987.
(37) Halgren, T. *Curr. Opinion Struct. Biol.* 1995, **5**: 205.
(38) Brooks, C. *Curr. Opinion Struct. Biol.* 1995, **5**: 211.
(39) Bashford, D.; Gerwert, K. *J. Mol. Biol.* 1992, **224**: 473.
(40) Sampogna, R.; Honig, B. *Biophys. J.* 1994, **66**: 1341.
(41) Gilson, M. *Curr. Opinion Struct. Biol.* 1995, **5**: 216.
(42) Honig, B.; Nicholls, A. *Science* 1995, **268**: 1144.
(43) Iwata, S.; Ostermeier, C.; Ludwig, B.; Michel, H. *Nature* 1995, **376**: 660.
(44) Oesterhelt, D.; Stoeckenius, W. *Nat. New Biol.* 1971, **233**: 149.
(45) Oesterhelt, D.; Stoeckenius, W. *Proc. Natl. Acad. Sci. USA*, 1973, **70**; 2853.
(46) Warshel, A.; Karplus, M. *J. Am. Chem. Soc.* 1974, **96**: 5677.
(47) Birge, R.R.; Schulten, K.; Karplus, M. *Chem. Phys. Lett.* 1975, **31**: 451.
(48) Warshel, A. *Nature* 1976, **260**: 679.
(49) Warshel, A. *Proc. Natl. Acad. Sci. USA* 1978, **75**: 2558.
(50) Korenstein, R.; Hess, B. *FEBS Lett.* 1977, **82**: 7.
(51) Váró, G.; Bryl, K. *Biochim. Biophys. Acta* 1988, **934**: 247.
(52) Balashov, S.P.; Litvin, F.F.; Sineshchekov, V.A. *Sov. Sci. Rev. D. Physiochem. Biol.* 1988, **8**: 1.
(53) Gergely, C.; Ganea, C.; Váró, G. *Biophys. J.* 1994, **67**: 855.
(54) Logunov, I.; Humphrey, W.; Schulten, K.; Sheves, M. *Biophys. J.* 1995, **68**: 1270.
(55) Warshel, A.; Chu, Z.T.; Hwang, J.-K. *Chem. Phys.* 1991, **158**: 303.
(56) Schulten, K.; Karplus, M. *Chem. Phys. Lett.* 1972, **14**: 305.
(57) Schulten, K.; Ohmine, I.; Karplus, M. *J. Chem. Phys.* 1976, **64**: 4422.
(58) Hudson, B.S.; Kohler, B.E.; Schulten, K. In *Excited States*; Lim, E.C., Ed.; Academic Press: New York, 1982; Vol. 6, p. 1.
(59) Tavan, P.; Schulten, K. *Phys. Rev. B.* 1987, **36**; 4337.
(60) Dinur, U.; Honig, B.; Schulten, K. *Chem. Phys. Lett.* 1980, **7:** 493.
(61) Schulten, K.; Dinur, U; Honig, B. *J. Chem. Phys.* 1980, **73;** 3927.
(62) Logunov, I.; Schulten, K. In *Quantum Mechanical Simulation Methods for Studying Biological Systems*; Bicout, D.; Field, M., Eds.; Springer: Heidelberg, 1996, pp. 236–256.
(63) Tavan, P.; Schulten, K.; Oesterhelt, D. *Biophys. J.* 1985, **47**: 415.
(64) Tavan, P.; Schulten, K. *Biophys. J.* 1986, **50**; 81.
(65) Humphrey, W.; Xu, D.; Sheves, M; Schulten, K. *J. Phys. Chem.* 1995, **99**: 14549.
(66) Fodor, S.P.A.; Ames, J.B.; Gebhard, R.; van den Berg, E.M.M.; Stoeckenius, W.; Lugtenburg, J.; Mathies, R.A. *Biochemistry* 1988, **2**: 7097.
(67) Smith, S.; Pardoen, J.; Mulder, P.; Curry, B; Lugtenburg, J. *Biochemistry* 1983, **22**: 6141.
(68) Smith, S.O.; Pardoen, J.A.; Lugtenburg, J.; Mathies, R.A. *J. Phys. Chem.* 1987, **91**: 804.
(69) Smith, S.O.; Hornung, I.; van der Steen, R.; Pardoen, J.A.; Braiman, M.S.; Lugtenburg, J.; Mathies, R. *Proc. Natl. Acad. Sci. USA* 1986, **83**: 967.
(70) Gerwert, K.; Siebert, F. *EMBO J.* 1986, **4**: 805.
(71) Grossjean, M.F.; Tavan, P.; Schulten, K. *Eur. Biophys. J.* 1989, **16**: 341.
(72) Engelman, D.M.; Zaccai, G. *Proc. Natl. Acad. Sci. USA* 1980, **77**: 5894.
(73) Trewhella, J.; Popot, J.L.; Zaccai, G.; Engelman, D.M. *EMBO J.* 1986, **5**: 3045.
(74) Popot, J.L.; Engelman, D.M.; Gurel, O.; Zaccai, G. *J. Mol. Biol.* 1989, **210**: 829.
(75) Papadopoulos, G.; Dencher, N.; Zaccai, G.; Buldt, G. *J. Mol. Biol.* 1990, **214**: 15.
(76) Heyn, M.P.; Cherry, R.J.; Muller, U. *J. Mol. Biol.* 1977, **117**: 607.

(77) Santarsiero, B.D.; James, M.N.G. *J. Am. Chem. Soc.* 1990, **112**: 9416.
(78) Nonella, M.; Windemuth, A.; Schulten, K. *J. Photochem. Photobiol.* 1991, **54**: 937.
(79) Zhou, F.; Windemuth, A.; Schulten, K. *Biochemistry* 1993, **32**: 2291.
(80) Smith, S.O.; Hornung, I.; van der Steen, R.; Pardoen, J.A.; Braiman, M.S.; Lugtenburg, J.; Mathies, R.A. *Proc. Natl. Acad. Sci. USA* 1986, **83**; 967.
(81) Schulten, K. In *Energetics and Structure of Halophilic Organisms*; Caplan, S.R.; Ginzburg, M., Eds.; Elsevier: Amsterdam, 1978, p. 331.
(82) Schulten, K.; Schulten, Z.; Tavan, P. In *Information and Energy Transduction in Biological Membranes*; Bolis, L.; Helmreich, E.J.M.; Passow, H., Eds.; Alan R. Liss: New York, 1984, p. 113.
(83) Humphrey, W.; Logunov, I.; Schulten, K.; Sheves, M. *Biochemistry* 1994, **33**: 3668.
(84) Doukas, A.; Pandi, A.; Suzuki, T.; Callender, R.; Ottolenghi, M. *Biophys. J.* 1981, **33**: 275.
(85) Hildebrandt, P.; Stockburger, M. *Biochemistry* 1984, **23**: 5539,
(86) de Groot, H.J.M.; Harbison, G.S.; Herzfeld, J.; Griffin, R.G. *Biochemistry* 1989, **28**: 3346.
(87) Dupuis, P.; Harosi, F.; Sandorfy, C.; Leclercq, J.M.; Vocelle, D. *Rev. Can. Biol.* 1980, **39**: 247.
(88) Cao, Y.; Váró, G.; Chang, M.; Ni, B.; Needleman, R.; Lanyi, J.K. *Biochemistry* 1991, **74**: 10972.
(89) Baasov, T.; Sheves, M. *Biochemistry* 1986, **25**: 5249.
(90) Gat, Y.; Sheves, M. *J. Am. Chem. Soc.* 1993, **115**: 3772.
(91) Maeda, A.; Sasaki, J.; Shishida, Y.; Yoshizawa, T. *Biochemistry* 1992, **31**: 462.
(92) Maeda, A.; Sasaki, J.; Yamazaki, Y.; Needleman, R.; Lanyi, J.K. *Biochemistry*, 1994, **33**: 1713.
(93) Ottolenghi, M.; Sheves, M. *J. Membr. Biol.* 1989, **112**: 193.
(94) Scharnagl, C.; Hettenkofer, J.; Fischer, S. *Int. J. Quantum Chem. Biol. Symp.* 1994, **21**: 33.
(95) Scharnagl, C.; Hettenkofer, J.; Fisher, S. *J. Phys. Chem.* 1995, **99**: 7787.
(96) Werner, H.-J.; Knowles, P.J. *J. Chem. Phys.* 1985, **82**: 5053.
(97) Knowles, P.J.; Werner, H.-J. *Chem. Phys. Lett.* 1985, **115**: 259.
(98) Birge, R.R.; Zhang, C.F. *J. Chem. Phys.* 1990, **92**: 7178.
(99) Schneider, G.; Diller, R.; Stockburger, M. *Chem. Phys.* 1989, **131**: 17.
(100) Govindjee, R.; Balashov, S.P.; Ebrey, T.G. *Biophys. J.* 1990, **58**: 597.
(101) Tittor, J.; Oesterhelt, D. *FEBS Lett.* 1990: **263**, 269.
(102) Doig, S.J.; Reid, P.J.; Mathies, R.A. *J. Phys. Chem.* 1991, **95**: 6372.
(103) Dobler, J.; Zinth, W.; Kaiser, W.; Oesterhelt, D. *Chem. Phys. Lett.* 1988, **144**: 215.
(104) Mathies, R.A.; Brito Cruz, C.H.; Pollard, W.T.; Shank, C.V. *Science* 1988, **240**: 777.
(105) Pollard, W.T.; Brito Cruz, C.H.; Shank, C.V.; Mathies, R.A. *J. Chem. Phys.* 1989, **90**: 199.
(106) Delaney, J.K.; Brack, T.L.; Atkinson, G.H.; Ottolenghi, M.; Steinberg, G.; Sheves, M. *Proc. Natl. Acad. Sci. USA* 1995, **92**: 2101.
(107) Xu, D.; Martin, C.; Schulten, K. *Biophys. J.* 1996, **70**: 453.
(108) Diller, R.; Stockburger, M. *Biochemistry* 1988, **27**: 7641.
(109) Eisfeld, W.; Pusch, C.; Diller, R.; Lohrmann, R.; Stockburger, M. *Biochemistry* 1993, **32**: 7196.
(110) Kalisky, O.; Ottolenghi, M.; Honig, B.; Korenstein, R. *Biochemistry* 1981, **20**: 649.
(111) Fahmy, K.; Siebert, F.; Grossjean, M.; Tavan, P. *J. Mol. Struct.* 1989, **214**: 257.
(112) Nagle, J.F.; Tristram-Nagle, S. *J. Membr. Biol.* 1983, **74**: 1.
(113) Gerwert, K. *Biochim. Biophys. Acta* 1992, **1101**: 147.
(114) Váró, G.; Lanyi, J.K. *Biochemistry* 1990, **29**: 6858.
(115) Váró, G.; Lanyi, J.K. *Biochemistry* 1991, **30**: 5016.
(116) Váró, G.; Lanyi, J.K. *Biochemistry* 1991, **30**: 5008.
(117) Xu, D.; Sheves, M.; Schulten, K. *Biophys. J.* 1995, **69**: 2745.
(118) van Laarhoven, P.J.M.; Aarts, E.H.L. *Simulated Annealing: Theory and Application*; Reidel: Dordrecht, 1987.
(119) Váró, G.; Zimanyi, L.; Chang, M.; Ni, B.F.; Needleman, R.; Lanyi, J.K. *Biophys. J.* 1992, **61**: 820.
(120) Takei, H.; Lewis, A. *Photochem. Photobiol.* 1993, **57**: 707.
(121) Sasaki, J.; Shichida, Y.; Lanyi, J.K.; Maeda, A. *J. Biol. Chem.* 1992, **267**: 20782.
(122) Metz, G.; Siebert, F.; Engelhard, M. *FEBS Lett.* 1992, **303**: 237.
(123) Subramanian, S.; Gerstein, M.; Oesterhelt, D.; Henderson, R. *EMBO J.* 1993, **12**: 1.
(124) Hauss, T.; Buldt, G.; Heyn, M.P.; Dencher, N.A. *Proc. Natl. Acad. Sci. USA* 1994, **91**: 11854.
(125) Ort, D.R.; Parson, W.W. *Biophys. J.* 1979, **25**: 355.
(126) Sheves, M.; Baasov, T. *J. Am. Chem. Soc.* 1984, **106**: 6840.
(127) Roepe, P.D.; Ahl, P.L.; Herzfeld, J.; Lugtenburg, J.; Rothschild, K.J. *J. Biol. Chem.* 1988, **263**: 5110.
(128) Noguchi, T.; Kolaczkowski, S.; Gartner, W.; Atkinson, G.H. *J. Phys. Chem.* 1990, **94**: 4920.
(129) Sawatzki, J.; Fischer, R.; Scheer, H.; Siebert, F. *Biophysics* 1990, **87**: 5903.
(130) Zinth, W.; Dobler, J.; Franz, M.A.; Kaiser, W. In *Spectroscopy of Biological Molecules—New Advances*; Schmid, E.D.; Schneider, F.W.; Siebert, F., Eds.; Wiley: New York, 1988, p. 269.
(131) Kalisky, O.; Goldschmidt, C.R.; Ottolenghi, M. *Biophys. J.* 1977, **19**: 185.
(132) Hofrichter, J.; Henry, E.R.; Lozier, R.H. *Biophys. J.* 1989, **56**: 693.
(133) Drachev, L.A.; Dracheva, S.V.; Kaulen, A.D. *FEBS Lett.* 1993, **332**: 67.

(134) Steinberg, G.; Sheves, M.; Bressler, S.; Ottolenghi, M. *Biochemistry* 1994, **33**: 12439.
(135) Tittor, J.; Schweiger, U.; Oesterhelt, D.; Bamberg, E. *Biophys. J.* 1994, **67**: 1682.
(136) Sperling, W.; Carl, P.; Rafferty, C.N.; Dencher, N.A. *Biophys. Struct. Mech.* 1977, **3**: 79.
(137) Sperling, W.; Rafferty, C.; Kohl, K.; Dencher, N. *FEBS Lett.* 1979, **97**: 129.
(138) Iwasa, T.; Tokunaga, F.; Yoshizawa, T. *Photochem. Photobiol.* 1981, **33**: 539.
(139) Bryl, K.; Taiji, M.; Yoshizava, M.; Kobayashi, T. *Photochem. Photobiol.* 1992, **56**: 1013.
(140) Zhu, Y.; Liu, R. *Biochemistry* 1993, **32**: 10233.
(141) Ferrand, M.; Zaccai, G.; Nina, M.; Smith, J.; Etchesbest, C.; Roux, B. *FEBS Lett.* 1993, **327**: 256.
(142) Nina, M.; Roux, B.; Smith, J. *Biophys. J.* 1995, **68**: 25.
(143) Levitt, M.; Sander, C.; Stern, P.S. *J. Mol. Biol.* 1985, **181**: 423.
(144) Sessions, R.; Dauber-Osguthorpe, P.; Osguthorpe, D. *J. Mol. Biol.* 1988, **209**: 617.
(145) Cartling, B. *J. Chem. Phys.* 1989, **91**: 427.
(146) Hu, Y.; Fleming, G.R.; Freed, K.F.; Perico, A. *Chem. Phys.* 1991, **158**: 395.
(147) Sessions, R.; Dauber-Osguthorpe, P.; Osguthorpe, D. *Biopolymers* 1993, **33**: 1423.
(148) Durup, J. *J. Phys. Chem.* 1991, **95**: 1817.
(149) Hao, M.; Harvey, S. *Biopolymers* 1992, **32**: 1393.
(150) Peskin, C.S.; Schlick, T. *Commun. Pure Appl. Math.* 1989, **42**: 1001.
(151) Nyberg, A.; Schlick, T. *Chem. Phys. Lett.* 1992, **198**: 538.
(152) Jensen, N.G.N.; Doniach, S. *J. Comput. Chem.* 1994, **15**: 997.
(153) Field, M.J.; Bash, P.A.; Karplus, M. *J. Comput. Chem.* 1990, **11**: 700.
(154) Bash, P.A.; Field, M.J.; Davenport, R.C.; Petsko, G.A.; Ringe, D.; Karplus, M. *Biochemistry* 1991, **30**: 5826.
(155) Berendsen, H.; Mavri, J. *J. Phys. Chem.* 1993, **97**: 13464.
(156) Warshel, A. *Computer Modelling of Chemical Reactions in Enzymes and Solutions*; Wiley: New York, 1991.
(157) Gao, J.; Xia, X. *Science* 1992, **258**: 631.
(158) Aquist, J.; Warshel, A. *Chem. Rev.* 1993, **93**: 2523.
(159) Nina, M.; Smith, J.; Roux, B. *J. Mol. Struc.* 1993, **105**: 231.
(160) Thompson, M.; Schenter, G. *J. Phys. Chem.* 1995, **99**: 6374.
(161) Logunov, I. Schulten, K. *J. Am. Chem. Soc.* Submitted for publication. [Beckman Institute Technical Report TB-95-23].
(162) Schulten, K. In *Quantum Mechanical Simulation Methods for Studying Biological Systems*; Bicout, D.; Field, M., Eds.; Springer: Heidelberg, 1996, pp. 85–118.
(163) Sheiner, S. *Adv. Biophys. Chem.* 1993, **3**: 119.
(164) Havelka, W.A.; Henderson, R.; Oesterhelt, D. *J. Mol. Biol.* 1995, **247**: 726.
(165) Hu, X.; Xu, D.; Hamer, K.; Schulten, K.; Kopke, J.; Michel, H. *Protein Science* 1995, **4**: 1670.